CHAPTER 13

PREPARATION AND CHARACTERIZATION OF $BiSbTe_3$ THIN FILMS

THERMOELECTRIC THIN FILMS

About 25 years ago, a requirement of energy sources with long life and low power arose from both military and medical applications (for instance cardiac pacemakers). It was a time of great hope in thermoelectrics and things like solar cells and lithium batteries had not been invented to this date. All kinds and shapes of thin film thermoelectric generators (TFTEG's) that are of interest today, had already been suggested during the early 1970s.

However they did not find their place in commercial applications. The reason for this was the relatively high power requirement of practical applications in the 1970s which were in the order of Milliwatts. Such requirements are easier to fulfill with conventional bulk TEG's or other power sources. Because of their radioactive fuel those TEG's were too dangerous and too expensive for a widespread nonmilitary application.

Today we have another situation. Typical power consumption of modern CMOS circuits is of the order of microwatts. A watch circuit needs only 5μW at 1.5 V! Such small amount of power could be supplied by TFTEG's using temperature differences of only a few degrees from their environment. There is no need of any fuel, therefore there are no limits for the lifetime. On the other hand, there is now a strong competition of two well-established technologies: solar cells and long life lithium batteries. Both are cheap and cover more than possible power range of TFTEG's. Thermogenerators would be superior to solar cells in such case when there is no light but a temperature gradient available. They are superior to lithium batteries when a lifetime of more than 5 to 10 years is required. In

addition, thermogenerators have advantage over batteries from the environmental point of view.

From these considerations it can be estimated that, TFTEG's supplying 10 to 100 μ W at a temperature difference of a few degrees is in growing need and can prove successful in the market.

Thermoelectric cooling devices are solid-state modules whose operations are inverse to those of thermocouples and function on the well-known principle of the Peltier effect. Thermoelectric cooling devices are quite reliable, having no moving parts, no liquid, no gases and no compressor. An additional factor in their favour is that the coefficient of performance is independent of the system size. This leads to fabrication of miniature low-capacity cooling devices, which are found in a variety of commercial, industrial, medical and laboratory appliances.

Recently, considerable efforts have been directed towards design and preparation of thermoelectric (TE) modules with high value of coefficient of performance[1]. In search of minimizing the dimension and cost of TE devices, thin film techniques have been investigated. Although thin film TE materials are very promising, their reproducible preparation is not easy especially in the case of multicomponent materials such as solid solutions of Bi_2Te_3, Sb_2Te_3 and Bi_2Se_3. Further, special features of the crystal structure of materials based on bismuth and antimony chalcogenides are the reason for a strong anisotropy of the thermoelectric properties of single-crystalline $(BiSb)_2(TeSe)_3$ films, a high strain sensitivity of polycrystalline films[2,3], and a strong dependence of the electrical properties of the films on the deposition conditions and subsequent heat treatment[4].

It is known that anomalously high elastic stresses are built up during condensation of films of certain materials. These stresses are due to the mismatch between the lattice parameters of the substrate and the film, presence of oxygen and other factors. Such stresses can alter significantly the energy band structure of a semiconductor and this can give rise to considerable changes in the electrical

properties. Gol'tsman et al[5] have determined the influence of mechanical stresses on the electrical conductivity and thermoelectric power in the films of $(BiSb)_2Te_3$ solid solutions. However, whatever method for preparation of thin film thermoelectrics is used, a subsequent annealing is inevitable to reduce defects and residual stresses introduced during fabrication processes and also to achieve uniform carrier concentration in the film.

The thermoelectric properties of as-deposited films of Bi_2Te_3 – based materials, however, are very poor, even if the overall stoichiometry is controlled. This is due to the residual stresses and local inhomogeneity in the composition of thin films. Therefore, adequate subsequent heat treatments are required to remove the defects. For Bi_2Te_3 – based thermoelectrics, it is necessary to anneal the thin films at 200 ~ 250 °C for about 3 hours to improve their properties comparable to those of bulk materials[6].

Hence the present study involves post deposition heat treatment and its effect on the electrical and optical properties of $BiSbTe_3$ films. The work carried out serves as preliminary investigation useful for development of thin film thermoelectrics.

THIN FILM PREPARATION TECHNIQUES

There are many deposition techniques for thin film formation. These techniques[7] have been broadly classified into four main groups.

1) Physical Vapor Deposition (PVD)
2) Chemical Vapor Deposition (CVD)
3) Electroless Deposition
4) Electrochemical Deposition

By combining PVD and CVD, hybrid techniques such as reactive evaporation/sputtering and plasma deposition have been established[8]. We will discuss some important techniques involved in the PVD since this technique has been used in this investigation.

Physical Vapour Deposition

This includes vacuum deposition techniques such as evaporation and sputtering. The main feature of these techniques is that the coating material passes through vapor phase by any one of the physical mechanism such as evaporation, sublimation or ion bombardment.

Thermal Evaporation:

In this PVD process, thermal evaporation is used to change the material to the vapour state. The material to be deposited, the evaporator and the substrate on which it is to be deposited are sealed in a chamber which is evacuated to the order of 10^{-5} Pa. The material to be evaporated is generally melted in a refractory filament or boat heated electrically under high vacuum. Evaporation from the melt of the material takes place and develops thin film on any obstruction placed in the path of substrate. The quality of thin film produced depends on

(a) purity and form of vaporising material

(b) cleaning and pretreatment of substrate material

(c) residual gas pressure and condensation rate.

Electron Beam Evaporation:

Some materials cannot be thermally evaporated because they have high melting points or because they will react with any material used to support them in the vacuum chamber thus making the deposited coatings contaminated. For such materials electron beam bombardment is used to raise the temperature of the evaporant. By controlling the kinetic energy of the electron beam, the depth of the melt area can be controlled. As a result the molten evaporant material does not come in contact and form alloy with the container or vessel. The advantages of this technique are:-

1) The coatings are purer,

2) High power available in the electron beam causes very high deposition rate possible, upto the order of 0.5 mm/min

3) In addition to Al and its alloys, other elements like Si, Pd, Au and dielectrics like Al_2O_3 can also be evaporated

Sputtering:

This technique is widely used due to its superiority over thermal evaporation and electron beam evaporation. In sputtering, high energetic ions are made to strike or bombard on the target surface, resulting in the removal of particles of atomic dimensions from the target. The material is thus removed in the form of atomic dimensions from the target and gets deposited on the substrate. The whole process of sputtering is carried out by discharge phenomenon. The major advantages of sputter deposition are:-

1) No critical vaporization temperature of the source material needs to be reached.
2) In alloy or compounds fractionation of the constituents does not take place and hence the original composition of the target material is conserved in the deposited thin film.

Investigations on sputtered V_2VI_3 semiconductor films are reported[9-12]. In all cases a lack of tellurium of several atomic % due to the different sticking coefficients of the elements was observed.

Stolzer et al[13] have described an experimental arrangement which combines the advantage of magnetron sputtering and the possibility of controlling the Te: (Bi, Sb) flux ratio.

Hot Wall Epitaxy (HWE) and Molecular Beam Epitaxy (MBE) Techniques :

These two techniques are a relatively new approach in thin film technology. Three temperature zone growth in vacuum is the basis for the development of hot wall epitaxy as well as molecular beam epitaxy techniques.

In order to improve the quality of epitaxial films of compound semiconductors, one approach which is very cost effective, is that of HWE, where the emphasis is put on the growth under conditions near thermodynamic equilibrium with minimum loss of material. The main feature of HWE is the use

of heated liner (hot wall) normally made up of a cylindrical quartz tube, which serves to enclose and direct the vapour from the source to the substrate. Thermal energy of the molecules is maintained with due exchange of heat energy with the wall through collisions in the course of evaporation and deposition. This avoids loss of evaporating material; the high vapour pressure of the constituents of the compound can be maintained and the difference between the substrate and source temperatures can be reduced to a minimum level. Molecules are made to travel linear paths inside the hot wall system by choosing the system design parameters so that when they reach the substrate they have a velocity component parallel to the surface, which in turn enhances their mobility along the substrate to locate their proper growth sites. This results in the formation of a defect free structure. Moderate vacuum of the order of 10^{-6} Torr is needed for the growth. This technique is capable of producing stoichiometric epitaxial film of high crystalline quality at comparatively low growth temperatures and in relatively short growth periods. The other advantage of HWE is the possibility of using the information contained in the phase diagram to determine not only the thermodynamic state of the evaporating source but also that of the vapour and the condensing materials.

Molecular beam epitaxy (MBE) has become a well established technique for the growth of ultra thin films with precise control of thickness, doping concentration and composition. It is a controlled thermal evaporation process under ultra high vacuum ($> 10^{-10}$ Torr) conditions. The technique gives high purity epi-growth. Relatively low growth temperature prevents interdiffusion. This leads to the formation of superfine structures with abrupt structural changes at the interfaces. Precise control over the incident beam fluxes and the relatively slow growth rates allow rapid changing of beam species, also take care of differences in the sticking coefficients and make possible the formation of structures of complex profiles in terms of both alloy compositions and/or impurity concentration.

Mzerd et al[14,15] studied molecular beam epitaxy of Bi_2Te_3 on Sb_2Te_3 crystals. They have found films to be nearly stoichiometric at substrate

temperatures 275°C ≤ T_s ≤ 325°C when using a very high oversupply of Te (R_f = 4.5).

Efforts for making smaller and highly-integrated thermoelectric modules have brought about new techniques for the preparation of Bi_2Te_3, PbTe, and $FeSi_2$ – based thin films; viz; sputter deposition[10,11], MOCVD[16], MBE[17,18], co-evaporation[19] and vacuum evaporation[7,20]. The Flash evaporation technique overcomes the difficulty posed by differences in volatility of the component elements in a compound/alloy material and has been successfully applied to prepare thin film thermoelectrics of good quality[21-24] The mixed crystal $(Bi_{0.25}Sb_{0.75})_2Te_3$ is known to be the best suited p-type material for thermoelectric devices like coolers or generators working near room temperature. There are some results published in recent years [25-27] about $(Bi_{0.25}Sb_{0.75})_2Te_3$ films having the same figure of merit viz., $3.10^{-3}K^{-1}$, as of single crystalline material. In these works the films have been produced by flash evaporation or hot wall epitaxy. These methods however have some disadvantages. Flash evaporation is difficult to control (therefore expensive) and as far as we know this process is not used in any industrial application. Hot wall epitaxy needs very high substrate temperatures, hence it excludes several substrate-materials.

The author has used thermal (direct) evaporation to obtain $BiSbTe_3$ thin films. The equipment used are described below. Also the conditions under which the thin film depositions were carried out for electrical and optical study are described below.

PHYSICAL VAPOR DEPOSITION UNIT

The actual vacuum coating unit[28] used for the preparation of $BiSbTe_3$ film is shown in Fig. 1. The assembly in the vacuum chamber is as required for thin film deposition by resistive heating method.

A substrate stand is provided to hold the substrate. The quartz crystal film thickness monitor is kept near the substrate to know the rate of deposition and thickness of the film being deposited. To fix the evaporation source, two metal

Fig. 1. Vacuum Coating Unit

electrodes are provided across which voltage is applied during deposition. The evaporation source and the substrate are kept in a straight line and the distance between them is normally about 20 cm.

A penning ionization gauge is connected to the chamber to measure vacuum and a pirani gauge in the backing line to sense the roughing pressure. The diffusion pump is connected directly below the chamber by a baffle valve. Rotary pump is placed away from the chamber via the roughing valve. The diffusion and the rotary pumps are connected by a backing valve. There is an air inlet valve to rotary pump which prevents the rotary pump oil from going into the chamber when the pump is closed and air is let in.

An air inlet valve is provided at the bottom of the chamber to break vacuum in the chamber. The dome of the chamber is made of stainless steel and gasket fitted to the base.

- **Vacuum Chamber**

The chamber gadgetory comprises of work holder ring which has a useful diameter of 8". The work holder ring is supported by three pillars fitted to the base plate. A standard filament holder is fitted to the L.T. live electrode and an earth electrode. The filament is normally positioned vertically below the centre of the work holder to give uniform distribution of vapours. A stainless steel wire mesh is fitted over the base plate to prevent foreign bodies falling into the baffle valve.

- **Vacuum Generation and Measurement**

For the preparation thin films, maintaining the vacuum in the chamber becomes an essential parameter. Vacuum affects the film growth in two ways:

a) It avoids oxidation and contamination of the film.

b) With decrease in pressure, sublimation time also decrease.

The oil sealed rotary pump gives vacuum upto 10^{-3} torr. The diffusion pump backed by the rotary pump gives vacuum of the order of 10^{-3} to 10^{-6}.

To measure vacuum attained in the vacuum chamber, the total gas pressure is the quantity most often used to characterize the degree of vacuum attained in a

system. For this purpose various gauges are available. There are two basic principles based on which such measuring of vacuum is done.

a) The direct measurement of pressure, i.e., force exerted per unit area.
b) The measurement of some physical property like thermal conductivity, resistance, degree of ionization of the gas as a function of gas density.

The vacuum gauges used in the present system were Thermocouple gauge/Pirani gauge and Penning gauge which work on second principle to measure the vacuum upto 10^{-3} torr and 10^{-6} torr respectively.

Thickness Measurement Techniques

While the various techniques commonly used for thickness measurement has been outlined below, the quartz crystal monitor has been used in the actual experiment. The various thickness measurement techniques commonly used are :

a) Weighing:

Assuming bulk density, the weight – thickness calibration charts are made which approximate the thickness of a thin film from its mass.

b) Stylus:

A stylus attached to a lever and fulcrum is made to traverse a substrate film step. The movement of the stylus is simplified and recorded.

c) Multiple Beam Interferometry:

The multiple beam interferrometric method has been extensively used for accurate thickness measurement. Sharp interference fringes are formed due to multiple reflections.

d) Beta particle back scattering:

Film thickness can be measured from the number of back scattered beta particle.

e) X-ray Fluorescence:

Secondary X-rays characteristic of the films are excited by primary X-ray directed onto the film. The intensity of the secondary X-rays are used to determine film thickness.

f) Tolansky Method:

In this method, multiple beam interferometry is adopted to determine the film thickness, by creating step when the film is partly removed by a sharp scalpel. From the fringes formed, step height is obtained as $h = (\lambda/2)dn$ with $dn = x/s$ where x is order of separation of fringes and s is the shift of fringes.

g) Quartz Crystal Monitor/ Digital Thickness Monitor:

The digital thickness monitor which is used by the author allows direct display of film thickness and rate of deposition during the evaporation. An oscillator quartz crystal with frequency of 6 MHz is positioned in the vacuum chamber so that vapour is deposited both on the substrate and defined area of the crystal. A second crystal (reference) having frequency of 6.4 MHz is positioned inside the monitor. The difference of 400 Hz initially is mixed with the output from a variable frequency oscillator to produce zero reading before each deposition. When deposition takes place on the crystal, a difference in the crystal frequency is created which is amplified and fed into a circuit where it is converted to a D.C. signal and the thickness of film is displayed on the monitor.

- **Source of Evaporation**

Temperature of a material for evaporation may be raised by direct or indirect heating. The simplest and the most common method is to support the material in a filament or a boat which is heated electrically.

A variety of sources are used to evaporate materials depending on whether they are available in wire, foil, ingot or compacted powder form and whether they react with the material or not. Many shapes and sizes of filaments and boats of a number of materials are available to suit a wide range of evaporation materials and applications. The most commonly used sources are W, Mo, Ta and other refractory materials. The sources used in this work were molybdenum boats.

- **Substrate for Deposition**

Various types of substrates are used for deposition of thin films. Commonly used materials are glass, mica, alumina etc. Stolzer et al.[26] have found polyimide (Kapton) foil to be a cheap substrate material that is of low thermal conductivity, chemically and thermally stable and has nearly the same thermal expansion coefficient as the $Bi_{0.5}Sb_{1.5}Te_3$ semiconductor. Gol'tsman et al.[5] have investigated the influence of mechanical stresses in films $(BiSb)_2Te_3$ prepared by thermal evaporation on to muscovite (mica) substrates. X-ray diffraction analysis showed that the films had single crystalline strucutre with the three-fold axis oriented normally to the substrate. The type of substrate to be used depends on the type of application. In the present work the $BiSbTe_3$ films were deposited on glass substrates for carrying out the electrical measurements and for obtaining x-ray diffractograms and on NaCl crystal for optical band-gap measurements.

(a) Preparation of substrate for deposition

Glass substrates have to be cleaned to remove grease, dirt etc. present on them. The substrates used are usually optically flat slides. For cleaning, the glass substrate is dipped into a detergent solution and both the surfaces cleaned. The glass substrates are then held under running water to remove the dirt, grease and the detergent solution. It is then dried with tissue paper and cleaned with cotton. The dry glass substrates are further cleaned with acetone and dried in an oven. While the glass substrate has been used for characterization and electrical study of $BiSbTe_3$ films, freshly cleaved NaCl crystals have been used for optical study since NaCl is transparent to infrared radiation. The NaCl crystal itself was affixed to a glass plate.

(b) Contacts for electrical measurements

The cleaned and dried glass substrates were deposited with thick coatings of silver (>1000 nm) at either ends for resistivity measurement. The glass substrate was masked in the centre with a 4 cm wide aluminium strip, so that only the two ends of the substrate are exposed to receive the Ag coating. Prior to deposition of

$BiSbTe_3$ film on these glass slides with Ag electrodes, a thick paper of the size 75mm × 25mm was taken and in the centre, a rectangular piece of the dimension 5mm width × 50mm length was cut out. The mask thus prepared allows films of dimensions 50 mm × 5 mm (l×b) to be deposited on the glass substrate with two ends of the films overlaying the Ag electrodes.

- **Heater for Annealing**

The heater used for annealing the films, was made in the laboratory. It is made of stainless steel cylinder having diameter 40mm and height 60mm. Kanthal wire which is insulated by porcelein beads was packed inside the cylinder with two leads of wire coming out. These two leads are connected to the variac to apply low voltage to heat the wire. The variac input voltage is so chosen that the glass substrate and the film are heated for annealing at desired temperature.

CHARACTERIZATION

In order to understand the film growth phenomena, two modes can be visualized. One, in which the film thickness increases as more and more material is deposited on it and second, in which grain growth and structural transformations takes place due to post deposition treatments. Transport properties of films of almost all materials are determined by the micro- and nano-structure evolved during condensation, nucleation and growth processes of impinging adatoms on a given surface. Hence structural characterization of the films is essential whenever any studies on them are to be carried out, irrespective of the nature of the properties. This is because of the fact that all the properties of thin films are controlled to a large extent – more so than in the case of bulk materials - by the structure of the films. The structure in general includes their crystal structure, micro-structure, defect structure and chemical composition. These would change with the changes in the film deposition parameters and also from method to method. As the structure itself changes, it is expected that the properties of different films should also be different. Hence the structural investigation of the

films whose properties are being studied is mandatory so that the data collected for the measurement of the properties are useful and reproducible.

Films of the solid solutions based on Bi_2Te_3 and Sb_2Te_3 are of interest as the starting point for the production of high-efficiency thin-film thermoelectric elements, radiation detectors, etc. Rajagopalan and Ghosh[29] reported electrical and thermoelectric properties of Sb_2Te_3 films deposited by a direct evaporation method. Patel and Patel[30] have reported optimization of growth conditions for Sb_2Te_3 films. Recently, Patel and Patel[31] have reported the variation of electrical and optical properties with the thickness of Sb_2Te_3 films. Patel and Patel[32] reported that Sb_2Te_3 films grown at 423 K by flash evaporation method are found to be single-phase polycrystalline, stoichiometric and to exhibit a minimum electrical resistivity. The thermoelectric properties of single-crystal and polycrystalline $Bi_{0.5}Sb_{1.5}Te_3$ films were investigated earlier[33] and data were obtained on the influence of the grain-boundary scattering of charge and heat carrier on the transport properties of these films. Gol'tsman and Komissarchik[5], Boikov et al.[34], and Lidorenko et al.[35] have studied the transport properties of thin films of solid solutions of antimony telluride and bismuth telluride. While there are a few reports on $Bi_xSb_{2-x}Te_3$ (x = 0.5) thin films [33-37], there is no report found, to the best of authors' knowledge, on the thin films with x = 1.

In the present case, thin films of $BiSbTe_3$ were thermally evaporated (as discussed above). Keeping other deposition conditions constant, films of different thicknesses were prepared, all at the rate of 0.8-1 nm/s. All the material placed in the source boat was evaporated to avoid chances of preferrential evaporation which would impair film composition. The films were then characterized by measuring the electrical and optical properties, while the structural informations were obtained from the X-ray diffraction analysis.

MICROSTRUCTURAL STUDIES

For the microstructural studies of the $BiSbTe_3$ thin films the deposition was made on thoroughly cleaned optical grade glass slides. The X-ray diffractograms of the thin films were obtained in the 2θ range of 15° to 60° using a Rigaku (Japan) Diffractometer (Fig. 2).

The X-ray diffractograms (Fig. 3) of the as-grown films of different thicknesses show that the films are polycrystalline in nature. It is further observed that the relative intensity peaks increase in their height and sharpness with increasing film thickness. This is due to improved crystalline perfection which can be explained as follows: In the early stages of growth the amorphous substrate surface causes heterogeneous nucleation. Hence at small film thicknesses there is poor crystallinity. With the increasing thickness, atomic arrangement in further layers gets gradually modified by the preceding layers which are far from amorphous. The nucleation of the progressively deposited layers are therefore less and less heterogeneous. This phenomenon tends to give preferred orientation to growth. Hence at higher film thicknesses beyond a certain limit, the crystallinity improves giving rise to higher and sharper peaks corresponding to the preferred orientation.

Fig. 4 shows the diffractogram pattern of an untreated and heat treated 174 nm film. It was observed that the peaks of the as-grown films for all thicknesses are not as prominent as in the case of heat treated films. This result indicates that heating improves the crystallinity, rendering the XRD peaks sharper and the excess Te in the films giving its prominent characteristic peak as observed in the pattern of the heat treated films (Fig. 4). This has its counterpart in electrical properties of these films discussed below. The diffraction pattern of the annealed and untreated films could be indexed on the basis of a rhombohedral unit cell. This was done using XRD POWD program (version 2.2). The 105 peak is common to both the annealed and as-grown films. Whereas, in the case of the annealed films, a new peak, viz., 110 appears (indicating improving crystallinity with annealing)

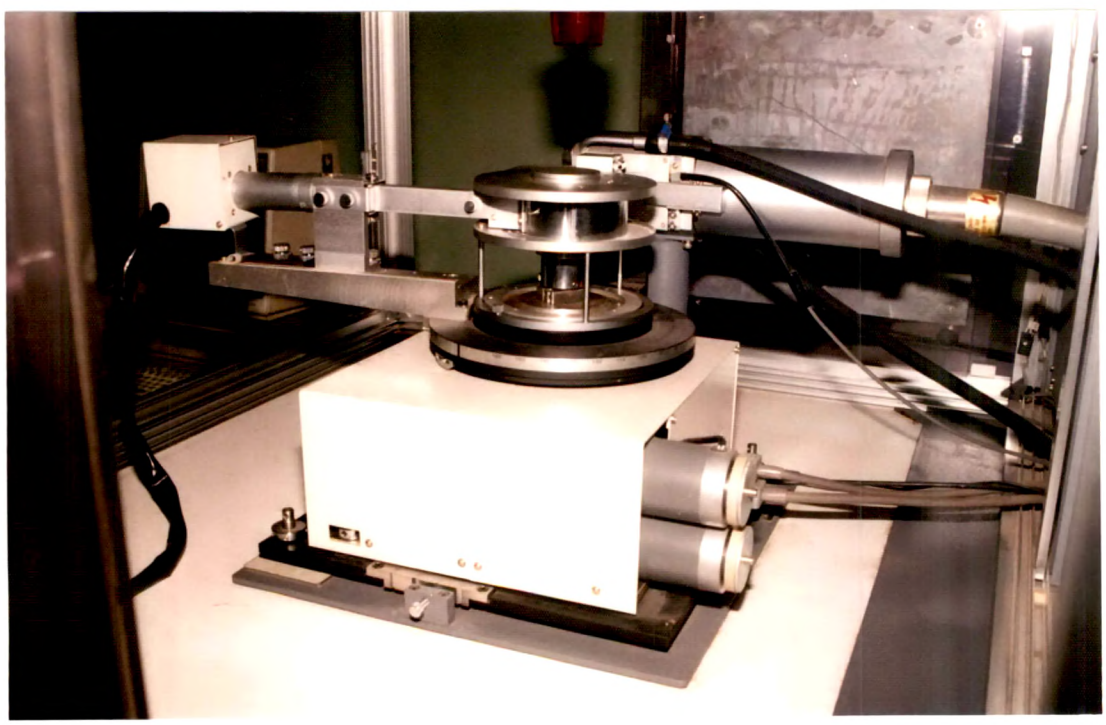

Fig. 2. Rigaku X-ray Diffractometer

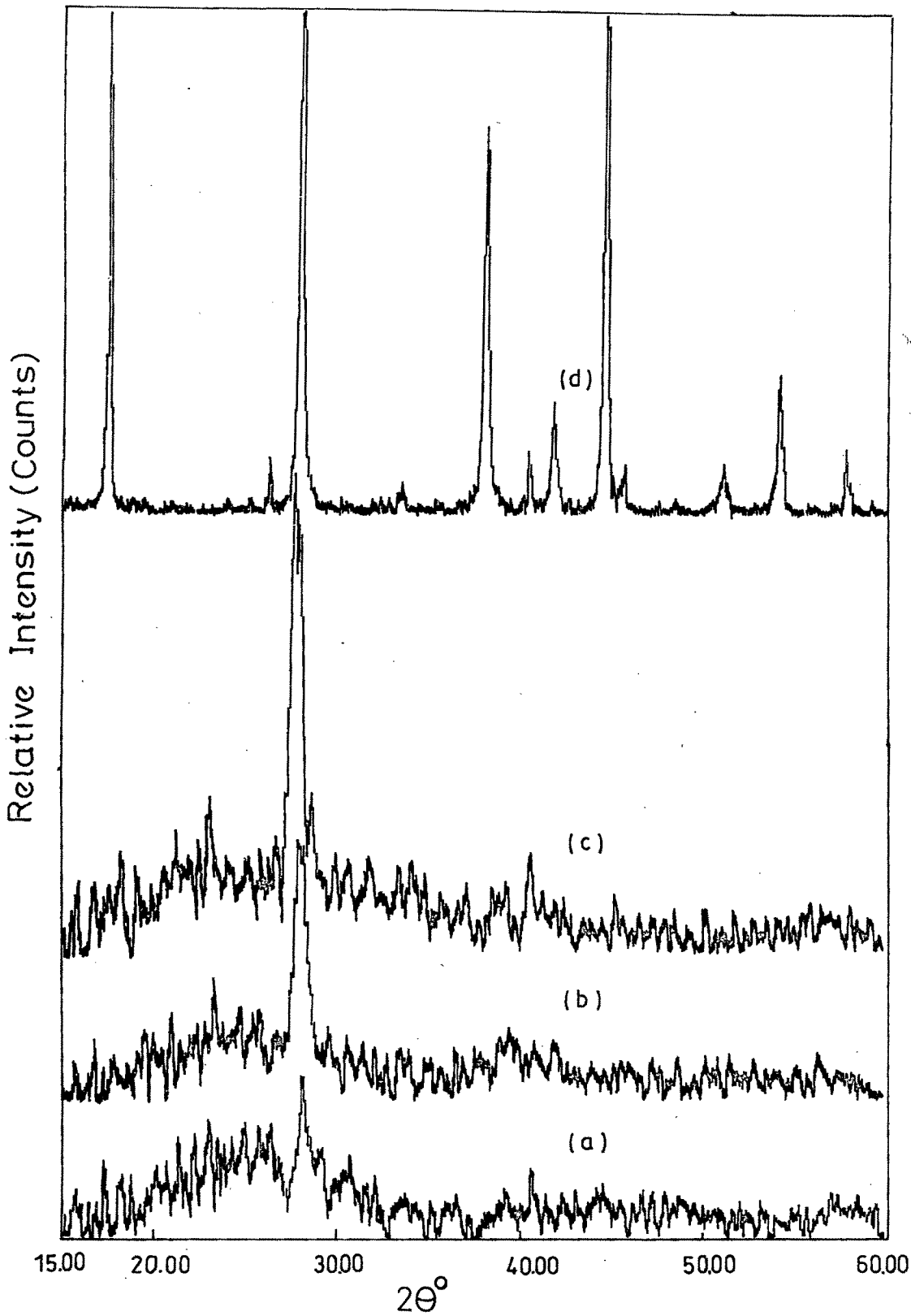

Fig.3 X-ray diffractograms of the as-grown $BiSbTe_3$ films (a) 61.5 nm (b) 174 nm (c) 272 nm (d) bull

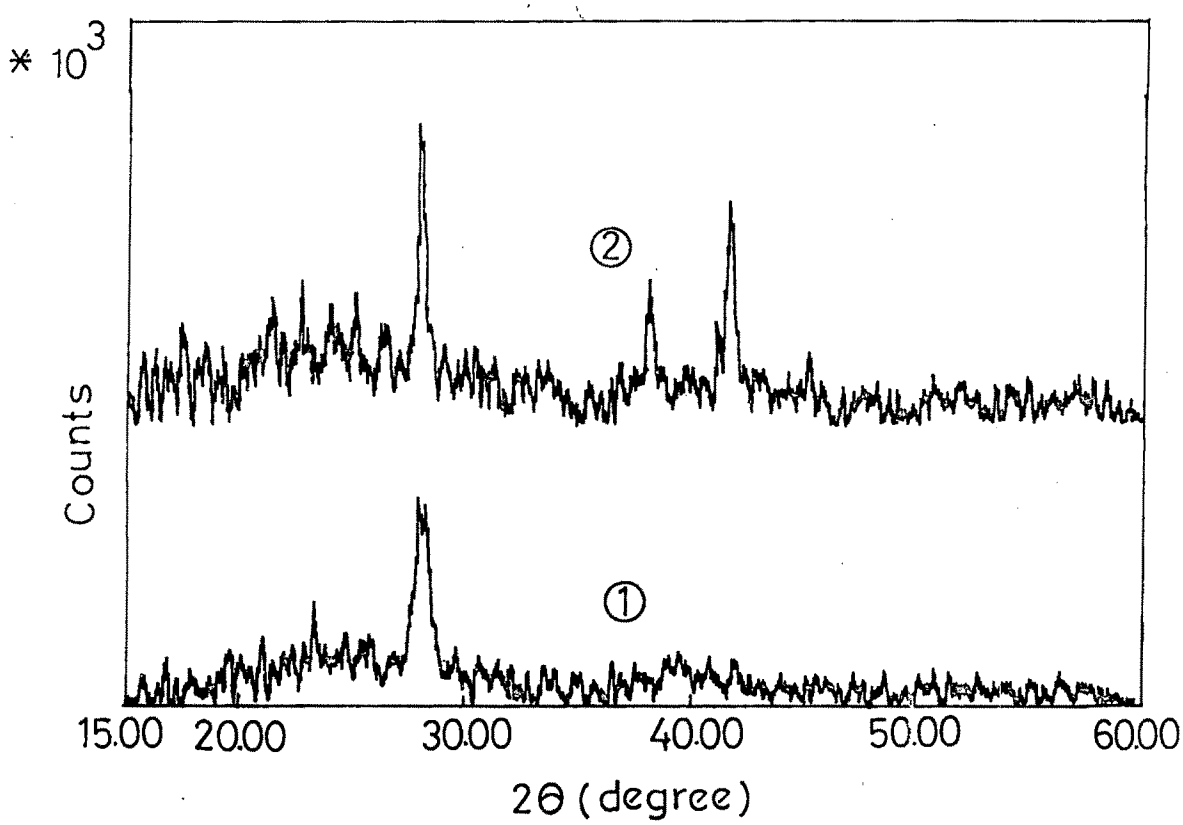

Fig.4 X-ray diffractograms of ① untreated and ② annealed thin films of $BiSbTe_3$ (1740 Å)

together with the free tellurium peak 102. The common occurrence of the 105 peak indicates the film to have a preference for (105) texture. In this context, it is interesting to note that in the study of texture and morphology of these films carried out by Stolzer et al.[26], the (105) texture has been reported to dominate when the substrate is non-crystalline. Their results are thus confirmed by the present observation. Additionally, it can be stated that this feature of (105) texture appears to be an inherent characterisitic of the material. This is so because in the x-ray powder diffraction results of this material (Chapter 9), among all peaks, the 105 peak is the most prominent one. The annealing treatment induces phase equilibria which corresponds to the bulk crystalline phase dominated by $BiSbTe_3$.

It is well known that the crystallite size D increases due to annealing[8]. This was evidenced by evaluating the crystallite size from the Full Width Half Maximum (FWHM) of the highest peak of the X-ray pattern of as-deposited and annealed films. The crystallite size D was evaluated using the Scherrer formula[38]

$$D = 0.94\ \lambda/\beta\cos\theta$$

where β is measured in radians at an intensity equal to half the maximum intensity (FWHM) , λ is the wavelength of the X-rays used and θ is the angle at which the intensity is maximum. It has been observed that annealing results in an increase of the grain size in the films. The crystallite size as evaluated using the Scherrer formula is given in Table 1 for the as-deposited and annealed $BiSbTe_3$ films. It is observed that the crystallite size variation has no definite trend with the film thickness. Nevertheless, the heat-treatment bears a pronounced improvement of structural perfection. Similar observations have been reported by Boikov et al.[33] for Bi_2Te_3 and $Bi_{0.5}Sb_{1.5}Te_3$ films.

ELECTRICAL PROPERTIES

The electrical resistivity measurements were made using the two probe technique. The details of the technique are given in Chapter 5. Thoroughly cleaned optical grade glass slides were used as substrates to deposit films of different

TABLE 1

Crystallite size of the as-deposited and annealed $BiSbTe_3$ thin films

Film Thickness (nm)	Crystallite Size (nm)	
	as-deposited	annealed
61.5	80	210
174	45	105
272	70	180

thicknesses at room temperature and thick silver films were used as electrodes. Electrical resistance of the film was measured in vacuum using Keithley Electrometer, model 614. The measurements were made at different temperatures at intervals of 2K between 290 and 450K. A chromel alumel thermocouple was used for the temperature measurements. The hot probe measurement of the films indicated the film conductivity to be p-type.

Fig. 5 shows the plot of resistivity versus thickness of the as-grown $BiSbTe_3$ films. The resisitivity is observed to decrease with increase in the film thickness. Fig. 6 shows the resistivity variation with temperature during heating and cooling in the case of an as-grown $BiSbTe_3$ thin film (thickness 102 nm). There is a significant rise of resistivity, by several orders of magnitude, above 330K, during the first heating. Upon cooling, the resistivity increases linearly. Thus it is evident that there is an irreversible change taking place in the film during the first heating. Such a change has been associated with amorphous-crystalline transition in the case of Sb_2Te_3 as reported by Damodar Das et al[39]. In the present case, the diffractograms obtained of as-grown films do not indicate amorphous nature of the films; they rather only show poor crystallinity. Nevertheless the first heating improves the crystallinity, rendering the XRD peaks sharper and the excess Te in the films giving its prominent characteristic peak as observed in the XRD pattern of the heat treated films (Fig. 4). This has its counterpart in Fig. 6 where we observe a decrease in resistivity with temperature, in the range from 296K to 330K indicating grain boundaries to bear important effect on the charge transport. Above 330K, the film properties start getting influenced by removal of excess Te to grain boundaries and to the surface, where these atoms become electrically inactive. Partial re-evaporation of tellurium from the surface takes place and structural changes occur. These effects lead to rise up in the resistivity. However, the resistivity approaches saturation soon beyond 400K. This behaviour can be associated with two counteracting phenomena: decrease in carrier concentration due to heat induced reduction in antisite defects

Fig. 5. Plot of resistivity versus thickness for $BiSbTe_3$ films deposited at room temperature

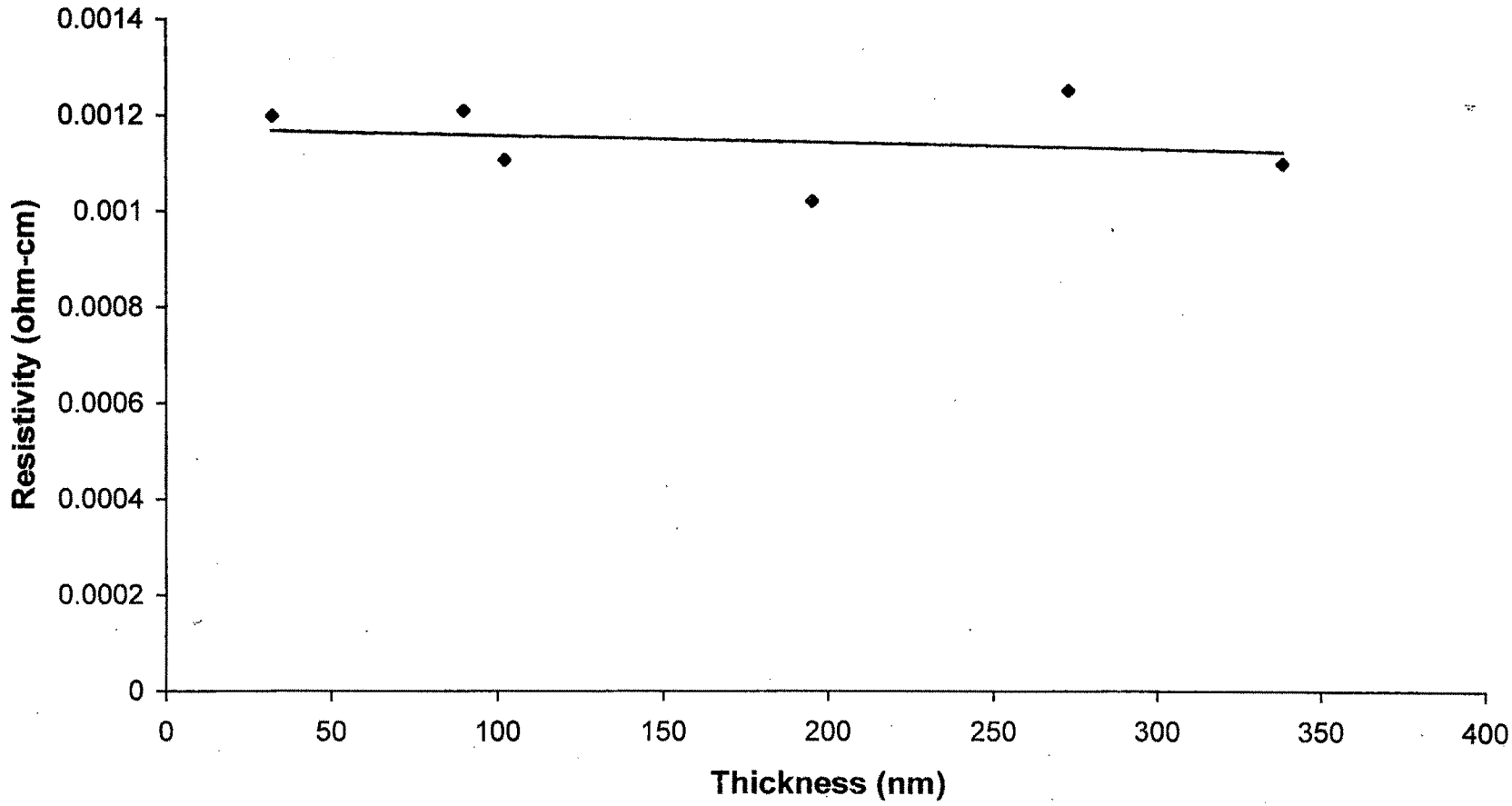

Fig. 6. Plot of Resistivity versus Temperature of 102 nm $BiSbTe_3$ thin film

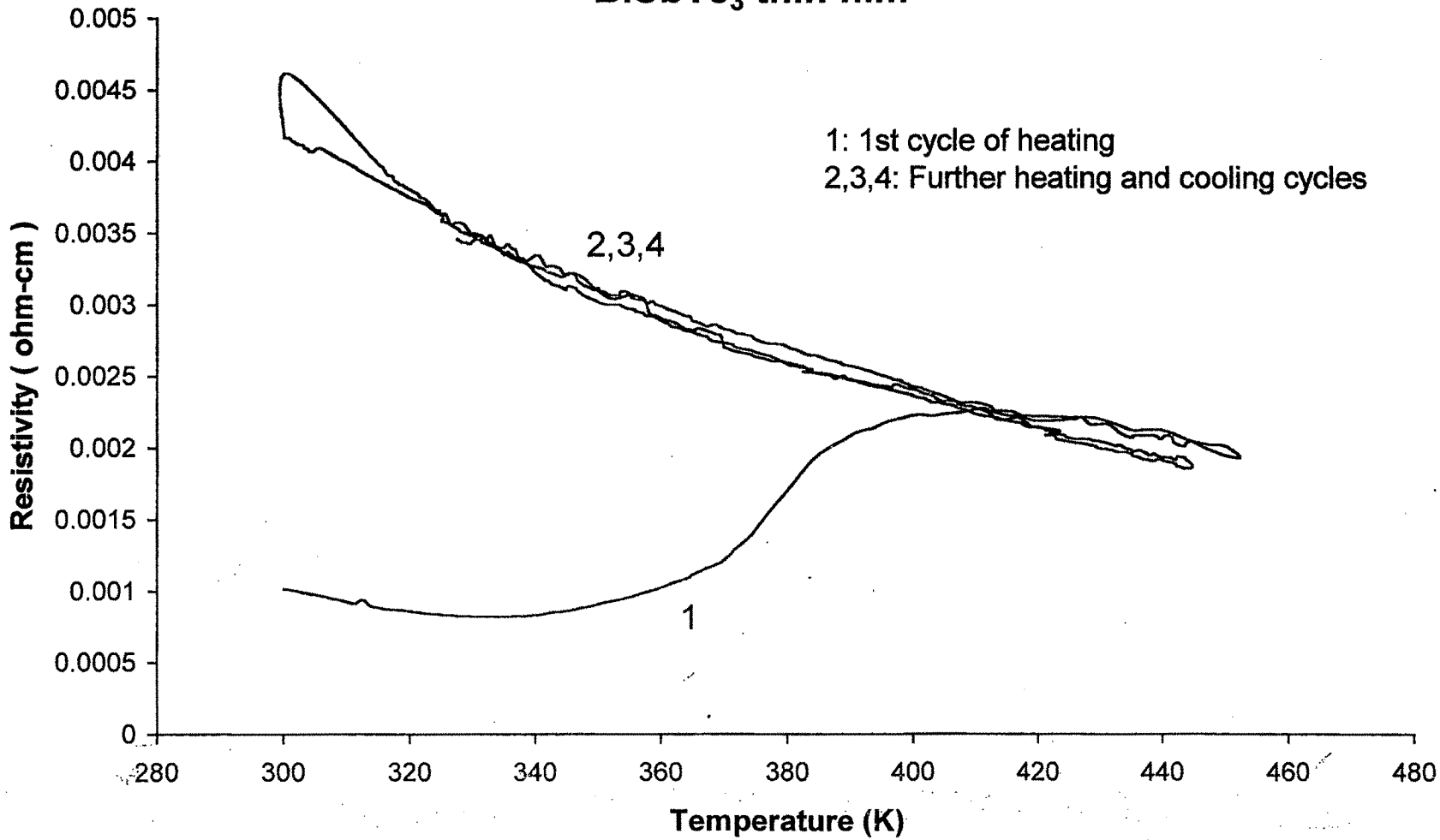

which in turn is compensated by increase in carrier mobility with improved crystallinity. Such trend of resistivity dependence on temperature for the first heating has also been reported for $Bi_{0.5}Sb_{1.5}Te_3$ thin films[37]. The resistivity measured in the successive heating and cooling cycles does not exhibit irreversibility (Fig.6), once the first heating has stabilized the films. The decrease in resisitivity with temperature in this case is the usual intrinsic semiconducting behaviour.

For further investigations, the films were annealed in vacuum at a pressure of 10^{-4} Pa at 400K for 1h. The results of resistivity measurements versus temperature for the further thermal cycles showed the resistivity decreases with temperature. Fig. 7 shows the plot of log ρ versus 1000/ T obtained for 102 nm $BiSbTe_3$ film. It is seen that the plot is linear. Similar plots were obtained for the films of other thicknesses. The slopes of the plots were used to evaluate the activation energies. Fig. 8 shows the plot of activation energy versus thickness. It is seen that the activation energy of the films moderately increases (from about 80 meV to 185 meV) with increase in thickness. This suggests that the film thickness influences the activation energy to some extent. This apparently is related to the grain size of the films as it is well known that the film microcrystallite size increases with increase in thickness upto the film continuity stage and thereafter remains almost constant.

OPTICAL BAND GAP

For the optical band gap study, films of different thicknesses were deposited on NaCl crystals and the IR absorbance spectra were obtained using an F.T.I.R spectrophotometer (BOMEM, Canada) in the photon energy range 0.06 – 0.5 eV. The details of the spectrophotometer used are given in Chapter 11. The optical absorption coefficient was calculated from the absorbance spectra at various incident photon energies. Fig. 9 shows the optical absorption coefficient of the as-deposited films of different thicknesses as functions of photon energy. The absorption coefficient has been observed to decrease with increase in the film

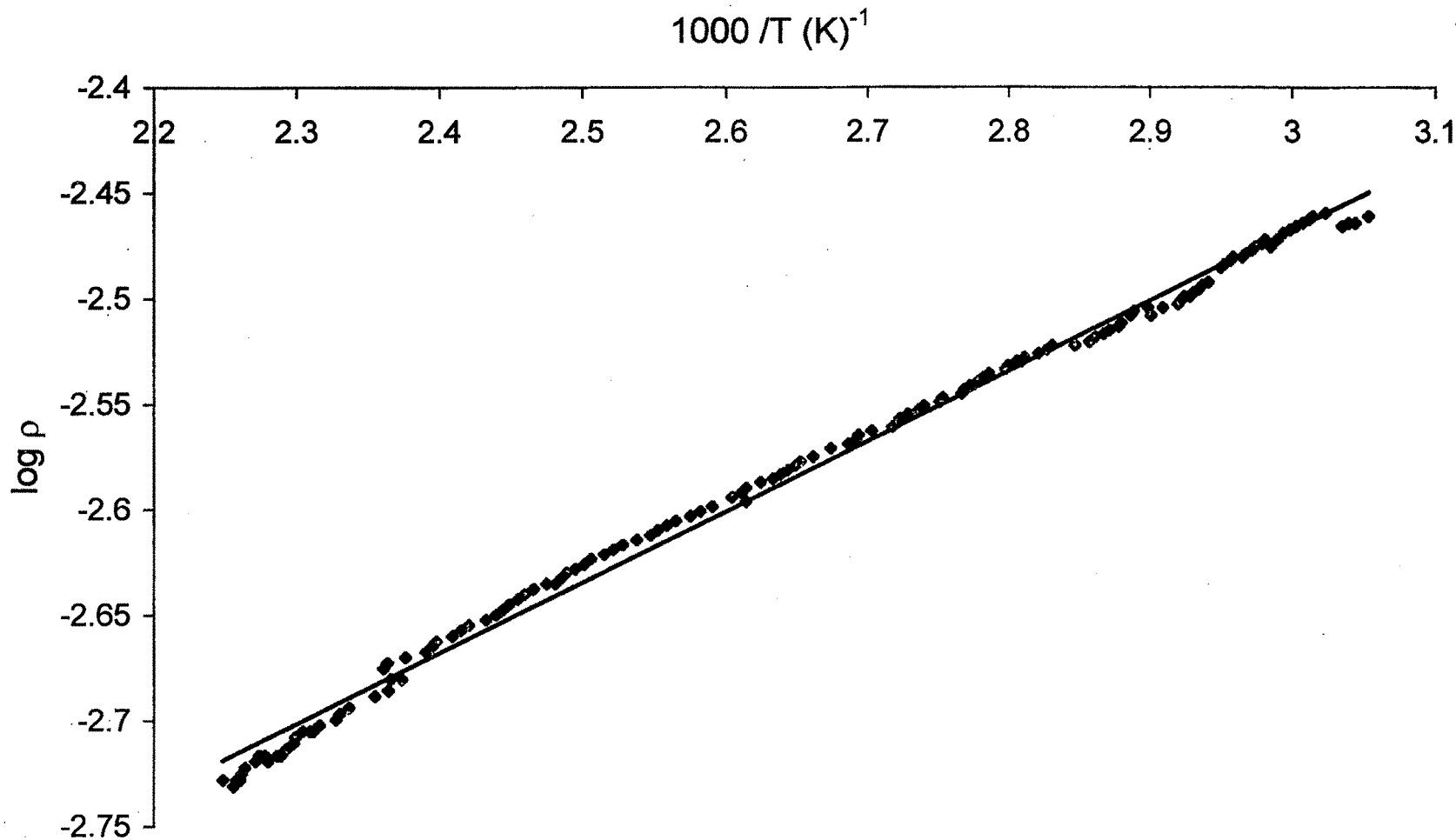

Fig. 7. Plot of log ρ versus 1000/T for 102 nm $BiSbTe_3$ film

Fig. 8. Plot of Activation energy versus thickness for $BiSbTe_3$ thin films

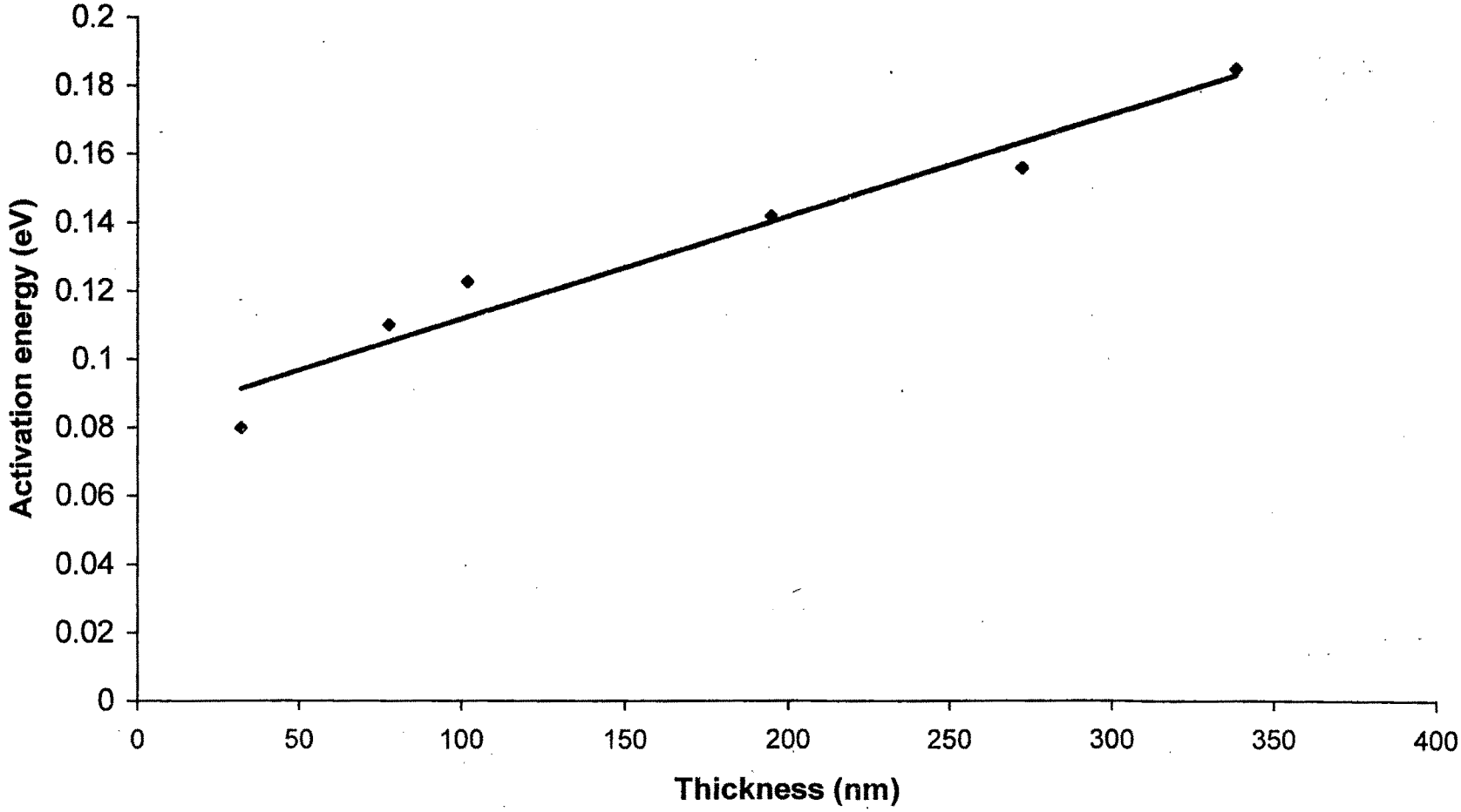

Fig. 9 Variation of absorption coefficient with incident photon energy of as-deposited films of different thicknesses.

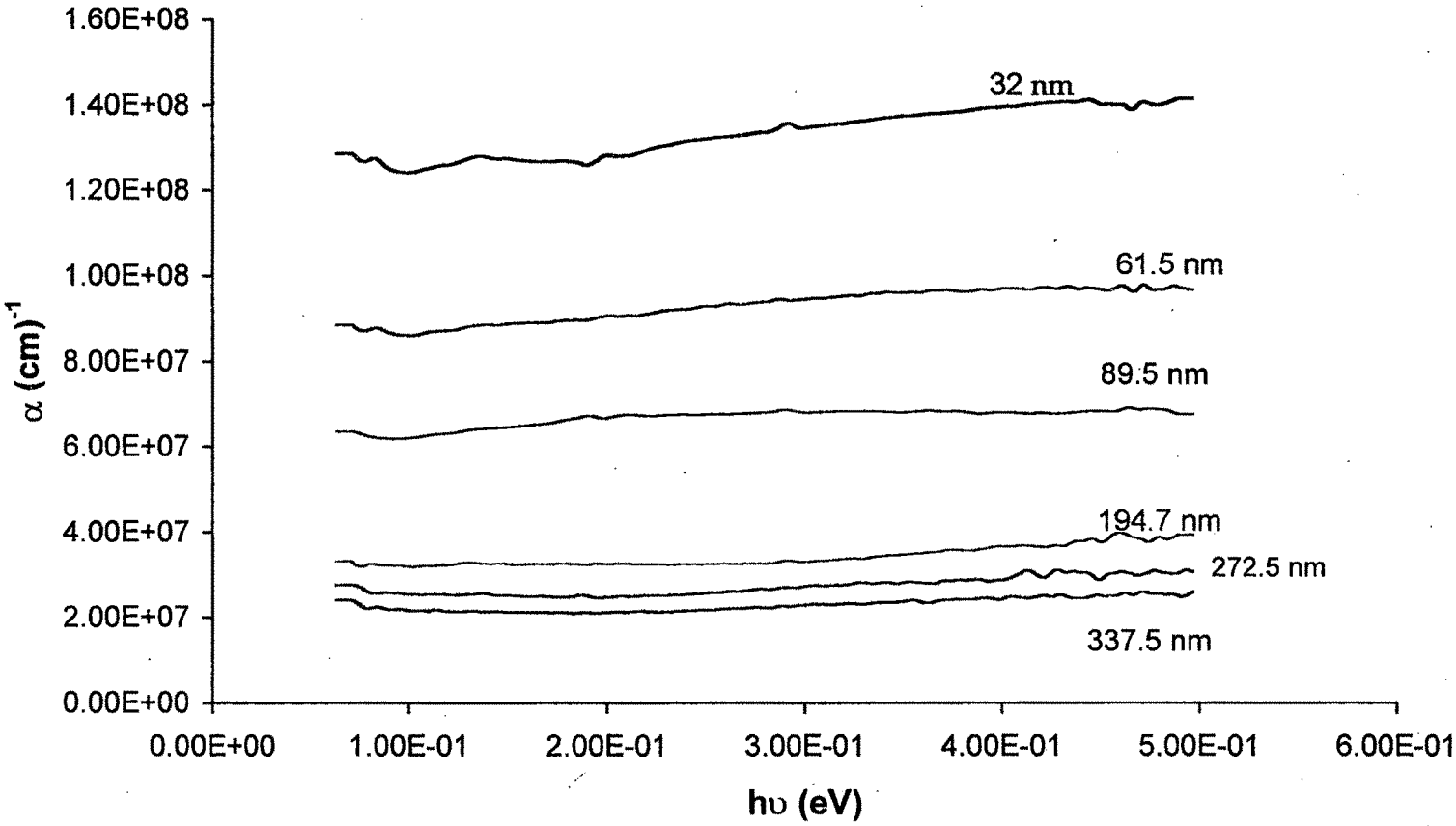

thickness indicating that the crystallinity changes considerably with thickness in the range 30 nm to 400 nm.

Figure 10 shows plots of $(\alpha h\nu)^2$ versus $h\nu$, where $h\nu$ is photon energy, α is absorption coefficient and h is Planck's constant, for the as deposited and annealed films, 174 nm thick. The variations are linear near the absorption edge indicating that absorption takes place through direct interband transitions. This can be described by the relation

$$\alpha h\nu = B\,(h\nu - E_g)^{1/2}$$

The energy of transition E_g, calculated from the above plots for the as deposited and annealed 174 nm film is given in Table 2. The band gap is observed to reduce by 5% on annealing.

The difference observed in the band gaps of the as-deposited and annealed films can be explained in terms of a change in barrier height due to a change in grain size in the polycrystalline film. According to the formula of Slater[40] and modified by Damodara Das and Jagdeesh[41], the barrier height E is given by

$$E = (N_0 e^2 / 4\pi k)\frac{[x - nD]}{N_0}$$

where e is the electronic charge, k is the dielectric constant of the material, N_0 is the density of charge carriers in the barrier, x is the thickness of the barrier, D is the average dimension of the crystallites and n is the density of electron-hole pairs created. The effect of these generated charge carriers is to reduce the barrier thickness and height by a constant factor (if n is constant at a given temperature). Thus it is seen from the above expression that the barrier height decreases as the crystallite size D increases. And as per our observations on the microstructural studies, the crystallite size increases on heat treatment. Thus annealing results in an increase of the grain size in the films which in turn reduces the band gap. Hence in the present observation, the decrease in the band gap with annealing is in

Fig. 10. Plots of $(\alpha h\upsilon)^2$ vs $h\upsilon$ for (1) as-deposited film and (2) annealed thin films of $BiSbTe_3$ (174 nm).

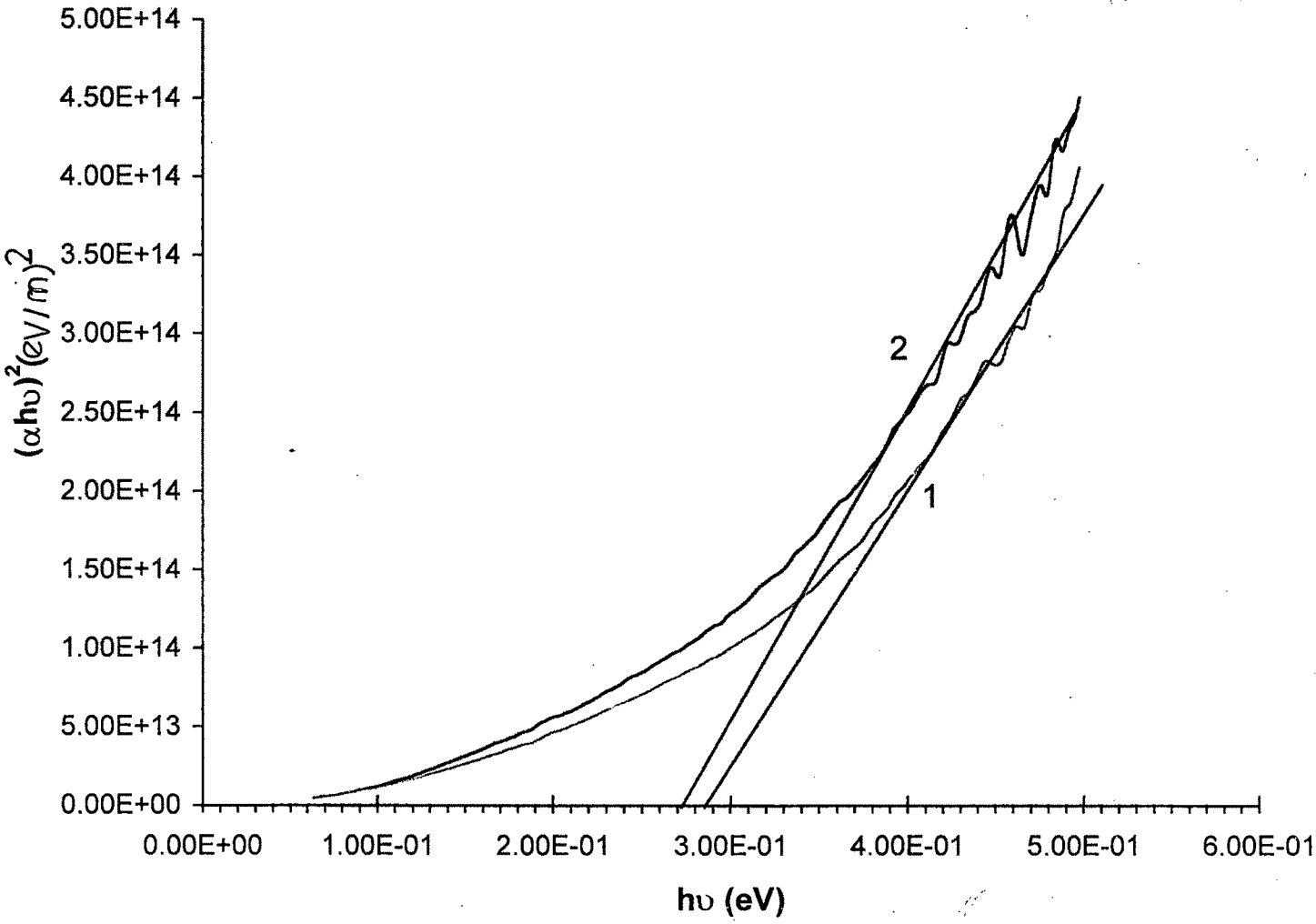

TABLE 2

Band gap of as-deposited and annealed $BiSbTe_3$ films

Film thickness (nm)	Band gap (eV)	
	as – deposited	annealed
61.5	0.220	0.205
174	0.285	0.270
272	0.255	0.240

agreement with the model of Slater. Further it has been observed that the effect of annealing reducing the band gap by 5% is similar for films of different thicknesses indicating that the crystallinity variation is also equivalent.

The band gap obtained for films of different thicknesses was found to exhibit no systematic dependence on thickness (Fig. 11), neither it is observed to remain constant with the thickness. The reason may be sought in the results of mass spectroscopy of these chalcogenides carried out by Borkowski et al.[42]. They report that at temperatures above 600°C at which these compounds normally evaporate, thermal dissociation as below takes place.

$Bi_2Te_{3/s/} \rightarrow 2\ BiTe_{/g/} + \frac{1}{2}\ Te_{2/g/}$

$Sb_2Te_{3/s/} \rightarrow \frac{1}{4}\ Sb_{4/g/} + SbTe_{/g/} + Te_{2/g/}$

Thus direct evaporation of $BiSbTe_3$ results in compositionally unstable vapour flux. Hence the films deposited in this way are not uniform with respect to composition. This probably explains the random variation of band-gap with thickness where the thickness itself is subdued as an effective parameter.

CONCLUSION

1) The thin films of $BiSbTe_3$ are semiconducting and p-type.
2) The resistivity of the films has but small linear dependence on film thickness with which it decreases.
3) The difference in resistance variation with temperature during the heating and subsequent cooling (and also heating) is attributed to the change in the tellurium concentration and hence the structural perfection.
4) The activation energy for conduction was calculated for different film thicknesses and it appears to be mildly thickness dependent.
5) Optical absorption measurements on the as-deposited and annealed $BiSbTe_3$ films indicate that the absorption is due to direct interband transition. Annealing of the films results in a decrease in the band gap energy due to an increase in the crystallite size as evaluated from the

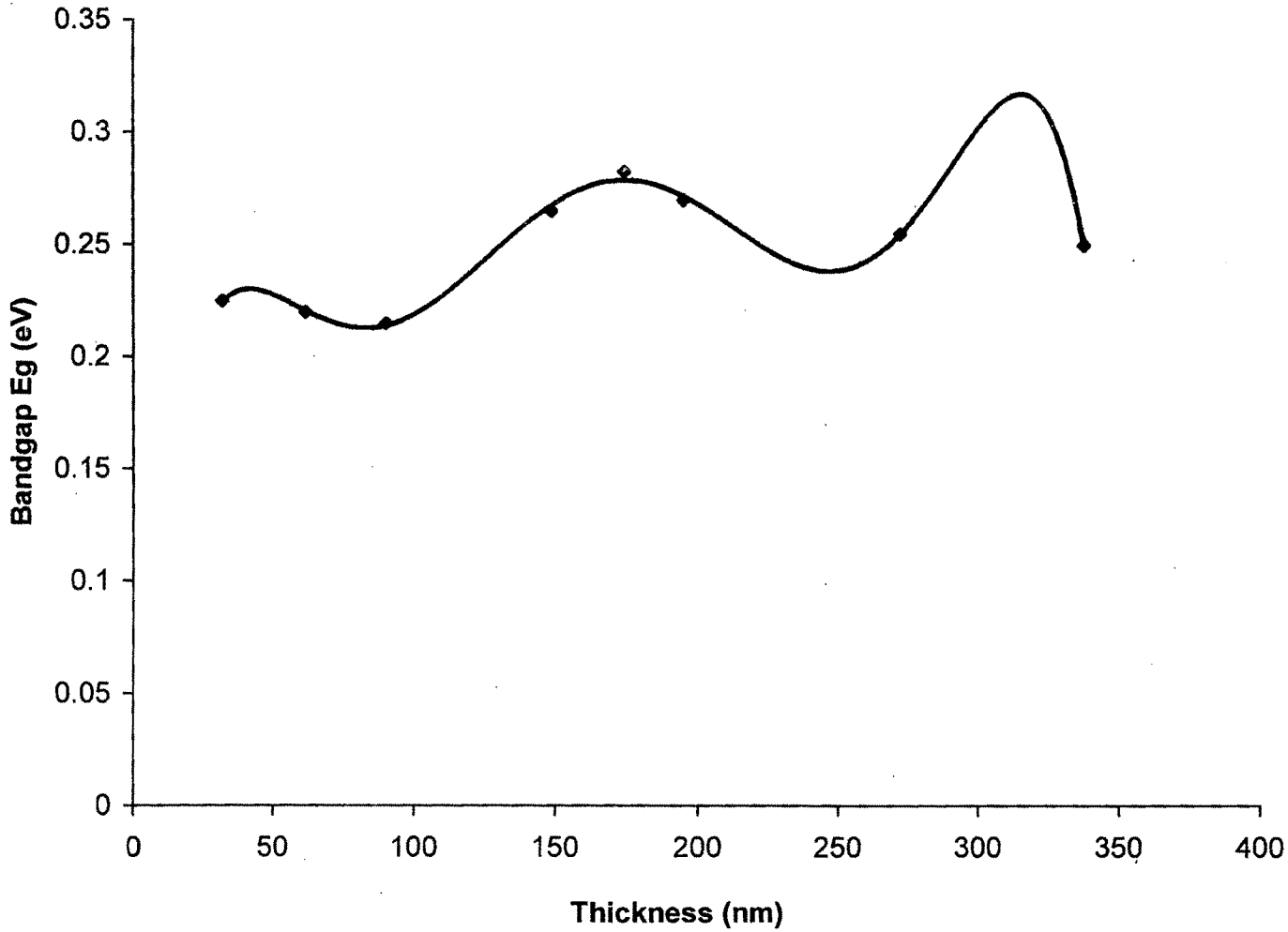

Fig. 11. Plot of Bandgap versus thickness for $BiSbTe_3$ films

FWHM of the highest peak of the X-ray pattern. This decrease is found to be independent of film thickness.

6) The film thickness dependence of optical band gap, if any, is obscured by compositional non-uniformity of the films.

REFERENCE

[1] Proc. Int. Conf. Thermoelectric Energy Conversion. (1980, 1982, 1984) Arlington, USA.

[2] Abduraimov, V. E., Boikov Yu. A. and Kutasov, V. A. (1984) Sov. Phys. Solid State. 26, 170.

[3] Atakulov, Sh. B., Azimov, T. and Shamsiddinov, A. N. (1982) Sov. Phys. Semicond. 16, 1326.

[4] Dashevskii, Z. M., Erusalimskaya, T. M., Kaller, Ya. A. and Kolomoets, N. V. (1976) Thermoelectric Materials and Films (in Russian) Institute of Nuclear Physics, Leningrad, 32.

[5] Gol'tsman, B. M. and Komissarchik, M. G. (1973) Sov. Phys. Solid State 15, 219.

[6] Kim, Il-Ho and Lee, Dong-Hi (1993) in Proceedings of the 12th International Conference on Thermoelectrics (ICT'93), Yokohama, Japan, 328.

[7] Chopra K. L. (1969) " Thin Film Phenomenon", McGraw Hill, New York.

[8] Chopra, K.L. and Das, S.R. (1983) Thin film solar cells, Plennum Press, New York and London.

[9] Stolzer, M., Bechstein, V. and Meusel, J. (1997) in Proceedings of 16th International Conference on Thermoelectrics (ICT'97), Dresden, Germany, 93.

[10] Shing, Y. H., Chang, Y., Mirshafii, A., Hayashi, L., Roberts, S.S, Josefowicz, J. Y. and Tran, N. (1983) J. Vac. Sci. Technol. 2, 503.

[11] Noro, H., Sato, K. and Kagechika, H. (1993) J. Appl. Phys. 73, 1252.

[12] Stolzer, M. and Stordeur, M. (1992) in Proc. of 11th International Conference on Thermoelectrics, Arlington, 260.

[13] Stolzer, M., Bechstein, V. and Meusel, J. (1996) in Proceedings of 15th International Conference on Thermoelectrics, Paradena, 422.

[14] Mzerd, A., Sayah, D.,Tedenac, J. C. and Boyer, A. (1994) J. Mat. Sci. Lett. 13, 301.

[15] Mzerd, A., Sayah, D.,Tedenac, J. C. and Boyer, A. (1994) J. of Cryst. Growth 140, 365.

[16] Boulouz, A., Giani, A., Delannoy, F. P., Foucaran, A. and Boyer, A. (1997) Proceedings of 16th International Conference on Thermoelectrics, Dresden, Germany, 167.

[17] Charles, E., Groubert, E. and Boyer, A. (1988) J. Mat. Sci. Lett. 7, 575.

[18] Kikuchi, S., Iwata, Y., Hatta, E., Nagao, J. and Mukasa, K. (1997) Proceedings of the 16th International Conference on Thermoelectrics, Dresden, Germany, 97.

[19] George, J. and Pradeep, B. (1984) Solid State Comm. 56, 117.

[20] Boikov, Y. A. (1989) in Proceedings of the 8th International Conference on Thermoelectrics, Nancy, 18.

[21] Gu, M. G., Lee, S. Y. and Lee, D. H. (1990) Korean Appl. Phys. 3, 73.

[22] Myoeng, J. M., Lee, S. Y. and Lee, D. H. (1990) Korean Appl. Phys. 3, 195.

[23] Lee, S. Y. and Lee, D. H. (1990) J. of the Korean Institute of Metals 28, 627.

[24] Lee, S. Y. (1990) Ph.D. Thesis, Yonsei University, Korea.

[25] Volklein, F., Baier, V., Dillner, U. and Kessler E. (1990) Thin Solid Films 187, 253.

[26] Stolzer, M., Stordeur, M. and Stark, I. (1995) Proceedings of the 14th International Conference on Thermoelectrics (ICT'95), St. Petersburg, Russia, 445.

[27] Boikov, Yu. A. Gribanova, O. S., Danilov, V. A. and Kutasov, V. A. (1990) Sov. Phys. Solid State, 32, 2056.

[28] Instruction manual, HINDHIVAC Vacuum coating unit Model 15 F6, Hind High Vacuum Co. (P) Ltd., Bangalore.